Caving 2022 - Y Potvin (ed.)

An effective numerical method to understand different aspects of cave preconditioning

D Elmo *The University of British Columbia, Canada*

K Farahmand *WSP-Golder, Canada*

S Rogers *WSP-Golder, Canada*

K Veltin *WSP-Golder, Canada*

J Lett *Newcrest Mining Limited, Australia*

Abstract

Full-scale forward geomechanical modelling of the caving process, remains problematic, challenging the key principles of numerical analysis applied to rock engineering problems: i) a model is not and cannot be a perfect imitation of reality; and ii) numerical modelling is driven by questions. This paper presents a simpler numerical solution that follows fundamental modelling principles, whereby simple models are used to analyse different aspects of a given problem and to determine which process need to be considered explicitly and which can be represented in an average way. Synthetic cave models (SCM) are introduced as a suitable modelling approach for optimising hydrofracturing design and draw strategy by investigating a range of possible scenarios. The SCMs can be considered a scaled down version of a large, although simplified, mine scale problem. In the current paper, we have used SCM at different scale in terms of the adopted width of the simulated undercut. All modelling scenarios consider the development of a relatively deep cave located at a depth of 1,400 m. Due to their simple and conceptual nature, these models allow us to analyse different aspects of cave mechanics, including cave initiation, cave propagation, effectiveness of preconditioning, draw sequence and caving rates.

Keywords: *block caving, preconditioning, numerical modelling*

1 Introduction

Development of modern cave mines has become more challenging as those mines target deeper orebodies. Empirical based design methods have been developed and calibrated against case histories in shallower and more jointed rock mass, where the mechanisms of caving are predominantly controlled by gravity-driven processes. Those methods are not applicable to stress-driven caving processes in more competent and massive rock masses. Differences are not confined to mechanisms alone, and the authors argue there is the need to revise rock engineering terminology. For instance, the term massive is typically used in rock engineering to refer to a rock mass with few and sparse discontinuities. This description seldom applies to the conditions encountered in deep cave mines (depth in excess of 1,000 m), with rock masses behaviour being controlled by the presence of complex veining systems rather than open joints and defects within an otherwise intact rock matrix (Brzovic & Villaescusa 2007). Current core logging practices and classification methods (e.g. RQD, Deere et al. 1969; RMR, Bieniawski 1989) are also clearly not applicable to those deeper rock masses, which further contributes to the limitations of using empirical methods to understand caving mechanisms for deep cave mines.

Application of advanced numerical models are therefore essential to adequately analyse and design different geotechnical aspects of cave mining (e.g. Vyazmensky 2008; Elmo et al. 2008, 2010; Sainsbury et al. 2011, 2018; Beck & Pfitzner 2008; Beck & Putzar 2011). Despite increased modelling ability, full-scale forward modelling of caving processes remains problematic. In the literature, numerical models either trade the lack of explicitly considering fracturing and comminution processes for a 3D continuum analysis under the assumption of the rock mass being an equivalent continuum media, or they do consider explicit simulations of fracturing and comminution processes but limited to 2D analysis. The discussion highlights the contrast of continuum versus discontinuum modelling and the question of whether continuum models can effectively capture dynamic continuum-to-discontinuum processes typical of cave mining (Shapka-Fels & Elmo 2022). The introduction of a 3D caving model being able to incorporate fracture mechanics principles to explicitly simulate fragmentation processes at the level required to define the amount of fines produced at the drawpoints, while at the same time including a detailed representation of the rock mass structural character and simulations of preconditioning scenarios, remains one of the greatest modelling challenges in caving geomechanics. The question arises whether reaching such a modelling complexity would be required. As discussed in Elmo et al. (2015) and Elmo & Stead (2021), many of the details of rock mass behaviour are unknown and unknowable; therefore, geomechanical models are constrained by the impossibility to reduce the uncertainty associated with data collection (geological uncertainty), modelling (parameter and model uncertainty) and persons (human uncertainty). To quote JL Borges (1946), a model is not and cannot be a perfect imitation of reality:

> *"[…] In that Empire, the Art of Cartography attained such Perfection that the map of a single Province occupied the entirety of a City, and the map of the Empire, the entirety of a Province. In time, those Unconscionable Maps no longer satisfied, and the Cartographers Guilds struck a Map of the Empire whose size was that of the Empire, and which coincided point for point with it".*

Therefore, modelling requires the real problem be idealised and simplified. An interesting discussion on the use of simpler methods as precursors to more complex numerical analyses, integrating engineering and philosophical aspects of rock engineering design, is given by Mitelman (2020). It is not possible to completely reduce uncertainty and the potential permeation of cognitive biases in the modelling process (Elmo et al. 2022), therefore we cannot claim that numerical models are capable of predicting future conditions. As discussed by Shapka-Fels & Elmo (2022), the objective of forward-looking models should not be to predict rock mass behaviour accurately and quantitatively, but rather to frame and classify rock mass behaviour under different conditions and different levels of uncertainty.

In the context of the discussion above, this paper presents a modelling approach that due to its 2D conceptual nature can efficiently analyse different aspects of cave mechanics including cave initiation, cave propagation, effectiveness of preconditioning, draw sequence, and cave rates.

2 Modelling motivation

Numerical modelling continues to play an important role in the design of cave mines, as mass mining involves complex processes that cannot be fully described by empirical methods. As discussed in Section 1, the scope of the model is not to represent such processes in their entirety, rather the objective is to determine which process need to be considered explicitly and which can be represented in an average way (Hoek 1999). The question of whether we should use 2D or 3D numerical analysis, finite element versus discrete element or other forms of numerical approaches generally produces opposite and dividing opinions, which, in the authors opinions, tend to culminate in a very unproductive debate. The authors acknowledge the limitations of using a 2D approach to study 3D problems. However, as discussed in Shapka-Fels & Elmo (2022), complex 3D models do not necessarily provide more accurate predictions than simpler 2D models, since neither 2D or 3D models alone can change the unknown and subjective nature of many geotechnical parameters. The model must be driven by questions and its purpose should be to further our understanding of the processes involved (Elmo et al. 2012). Those are the metric that should be used to define the effectiveness of a model.

The numerical platform used in this paper is a finite discrete method (FDEM) approach incorporating fracture mechanics principles (ELFEN, www.rockfield.co.uk). Despite the approach offering a full 3D dimensional capability, this paper makes use of its 2D version to fulfil the requirement of performing a preliminary sensitivity analysis of key aspects of cave mechanics, by running multiple fracturing (discrete) models at a fraction of the computational cost of a single 3D continuum model. Earlier examples of cave modelling using the same FDEM platform are presented in Pine et al. (2007), Elmo et al. (2008, 2010) and Vyazmensky et al.

(2009a, 2009b). Details of the numerical formulation of the FDEM approach used in this paper are given by Owen et al. (2004), Pine et al. (2007) and Elmo et al. (2012).

3 Finite discrete method analysis of different preconditioning strategies

3.1 Model set up

Preconditioning by means of horizontal hydrofractures (not always horizontal fractures, depends on the stress orientations) is a technique used in cave mining to primarily reduce the magnitude of large seismic events and secondly improve rate of caving and to reduce the risk of cave stalling and hang-ups. It is very important to evaluate different preconditioning scenarios in terms of both operational limitations and geological constrains. This paper addresses those questions using a series of 2D cave models with the objective to characterise rock mass response, cave initiation and cave advance for varying preconditioning strategies. The models are defined synthetic cave models (SCM) and they represent a an undercut and height of the orebody of 177 m and 200 m, respectively. Despite their name, these are full-scale cave models, simulating extraction at a depth of 1,450 m; the models therefore focus on stress-driven caving rather than gravity-driven caving mechanics. Pre-mining stress is defined by a depth dependent stress ratio *k* (horizontal stress to vertical stress ratio).

Undercutting and draw is modelled using the same approach described in Elmo et al. (2010) and Shapka-Fels & Elmo (2022). Ore is removed across the assumed production level using a specific algorithm that removes all the meshed elements whose centroids are located within a specified region, and in this case corresponding to the undercut level. Ore is removed continuously at a given numerical time step in order to return the specified draw rate, and the model is calibrated to yield a draw rate of approximately 100 mm/day. This is illustrated in Figure 1. The approach offers a way to control the draw rate, which can then be related to the simulated caving rate. These models are not designed to simulate cave breakthrough to surface, and the simulation is terminated once a target height of draw (HOD) is reached. Compared to much larger cave-scale models, the SCM approach offers advantages in terms of run times, and several HF scenarios and draw strategies can be easily implemented and investigated (Table 1 and Figure 2). Whereas the HF scenarios are conceptual in nature, the material properties and pre-mining stress used in the models reflect conditions encountered at an undisclosed operating mine in Australia.

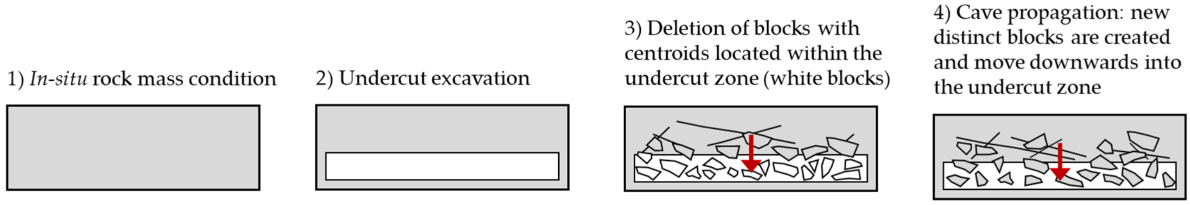

Figure 1 Illustration showing the four steps used to simulate ore removal and draw simulation

Table 1 Preconditioning scenario used in the analysis

Model type	H_L_H	H2_L_H2	HTP_L_HTP	L2_L_L2
Flank HF spacing/length	1.5 m/60 m	1.5 m/60 m	1.5 m tapered/60 m	3.0 m/60 m
Core HF spacing/length	3.0 m/80 m	3.0 m/80 m	3.0 m/80 m	3.0 m/80 m
Flank/core height	200 m/200 m	200 m/100 m	200 m/200 m	200 m/100 m
Weighted areal fracture Intensity for HF (m/m^2)	0.53	0.33	0.43	0.24

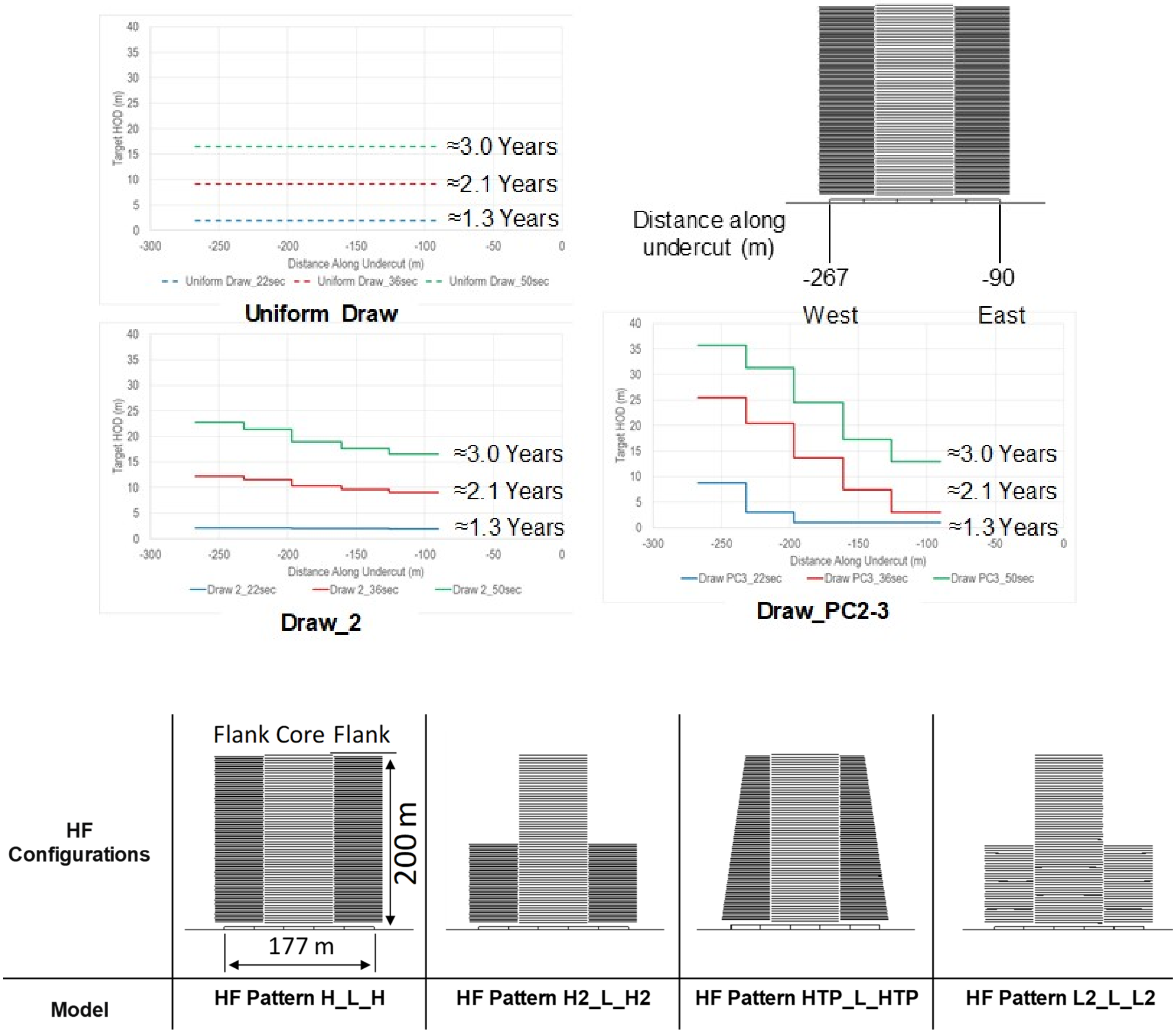

Figure 2 Draw strategies and geometry of preconditioning scenario used in the analysis. The hydrofracturing (HF) Pattern HTP_L_HTP is not realistic from an operation perspective; it is included only for comparison purposes

3.2 Modelling results

Figures 3 to 7 show the cave shapes at approximately 2.1 and 3.1 Years of real time for the 15 different models. Note that equivalency between modelling steps and real time was based on caving models developed for an existing cave mine (Rogers et al. 2014). For each model, the vertical displacement plots (note y-axes being in reverse order, negative displacement plotted upwards) for a series of history points above the undercut and the simulated cave shape are presented. Examining the shapes of the vertical displacement profiles for four different levels above the undercut (50 m, 100 m, 150 m, and 200 m) offers the opportunity to better understand the cave development under a specific combination of the imposed draw sequence and HF pattern. Note that the displacement profiles do not represent cave shapes. The displacement profiles only show the relative movement of a series of points at given elevation within the cave and provide an indirect indication of cave aspect (e.g. symmetrical versus asymmetrical). For example, leaning of a displacement profile towards the east or west of the undercut centre line could indicate the asymmetrical evolution of the cave due to a specific HF configuration and/or draw strategy. Additionally, the formation of a large gap between displacement profiles could be considered as an indication of reduction of caving rates and the initiation of a possible cave stall at a certain level above the undercut. Equally spaced displacement profiles for different levels would be an indication of a continuous caving process. The following observations are made with reference to Figures 3 to 7:

- Models with no HF: Figures 3a and 3b show that caving is marginally influenced by draw sequence up to 2.1 years of production when 'Uniform Draw' or 'Draw_2' strategies are applied. This can be inferred from the shape of the modelled caves shown in Figure 3a and 3b. In contrast, implementing an aggressive draw (PC3_Draw) on the west of the undercut leads to an asymmetrical cave development by Year 2.1, which further continues by Year 3.1. By then, deformations become more pronounced on the east due to a 'failed hanging wall' scenario, whereby the rock mass on the east flanks rotates and fails into the cave. The shape of the displacement profiles at 150 m and 200 m above the undercut suggests that a plug flow type of behaviour is generally absent.
- Models with H_L_H Pattern: Figure 4 (top images) shows that by Year 3.1, cave initiation and development in models with a high HF density in the flanks and low HF density in the core is only marginally influenced by the assumed draw sequence. Limited difference is observed between the Uniform Draw or Draw_2 strategies. The model with the more aggressive draw on the west side (Draw_PC3) shows an asymmetrical displacement profile limited to the initial 50 m above the undercut. The extent of the HF pattern appears to laterally bound the cave independently of the assumed draw strategy.
- Models with HTP_L_HTP Pattern: Figure 5 shows that the modelled response in the presence of tapered HF is influenced by the assumed draw sequence only for the case of an aggressively asymmetrical draw (Draw_PC3). By Year 3.1, the same cave height is achieved in the three models; however, the conclusion cannot be that the same caving rate is achieved independently of the assumed draw sequence, since the measurement of caving rate is subjective to the number of active points used in the calculation. The displacement profiles would suggest that a plug flow effect is present for Uniform Draw and Draw_2 scenarios, with more tonnes being pulled compared to the Draw_PC3 scenario. It is important to note that the combination of tapered HF pattern and asymmetrical draw strategy may cause a reduction in caving rates and 'necking' of the cave shape that could have an impact in terms of dilution and ore recovery.
- Models with H2_L_H2 Pattern: this model introduces a differential preconditioning strategy, whereby HFs are generated on the flanks but up to a height that is half of that of the preconditioned core. As shown in Figure 6, this strategy may have a detrimental impact on cave development, depending on the assumed draw sequence. For instance, a condition of cave stall is generated in an otherwise caveable rock mass by preferentially channelling the cave through a preconditioning core. For the models with Uniform Draw and Draw_PC3, cave propagation stalls approximately 150 m above the undercut. The modelling results demonstrate that the risk of cave stall could be prevented by using a less aggressive asymmetrical strategy such as Draw_2, while at the same time yield relatively high rates of caving. For the model with the Draw_PC3 draw sequence the condition of cave stall has disappeared by Year 3.1 as the model continues to pull more material asymmetrically from the west side.
- Models with L2_L_L2 Pattern: this model introduces a modified differential preconditioning strategy, whereby HF are generated on the flanks but up to a height that is half of that of the preconditioned core and with a reduced intensity. As shown in Figure 7, when combined with a uniform draw strategy the modified differential preconditioning strategy leads to a cave stall condition approximately 100 m above the undercut. However, this condition is not present for asymmetrical draw sequences. While the Draw_2 strategy leads to a relatively symmetrical cave devolvement, the Draw_PC3 strategy appears to prevent the cave from growing vertically upwards and eventually causes the cave to lean towards the east side.

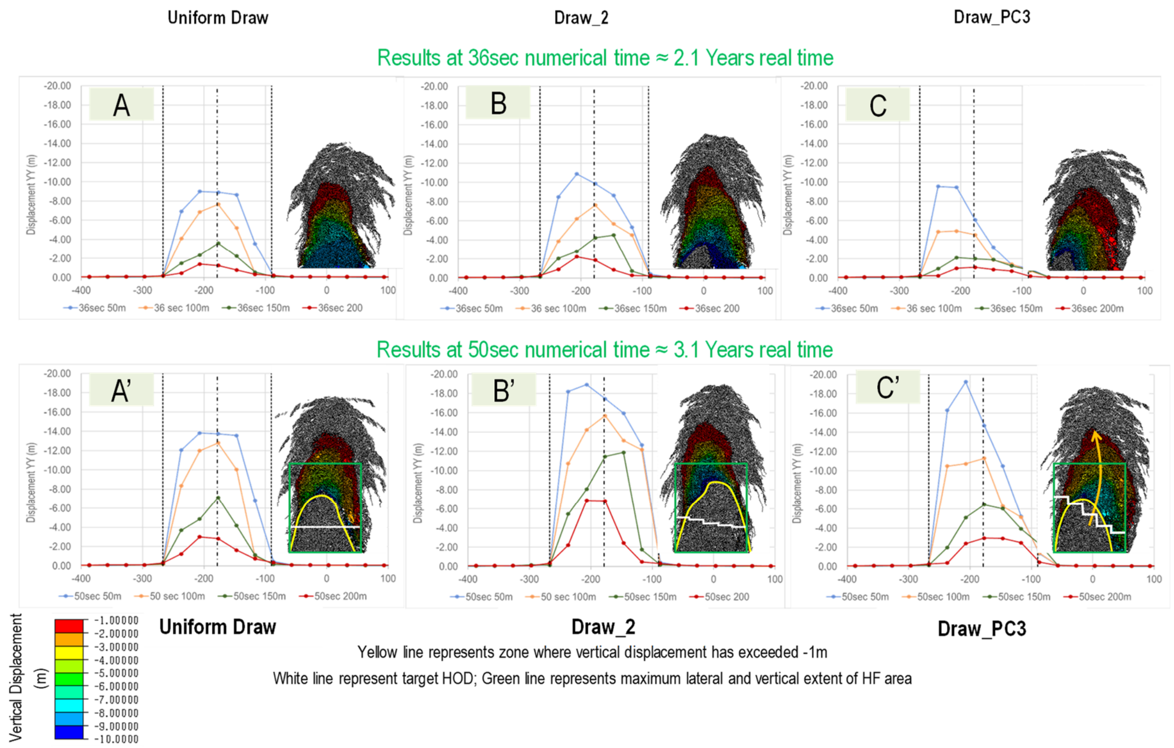

Figure 3 Vertical displacement plots for the cave model without preconditioning

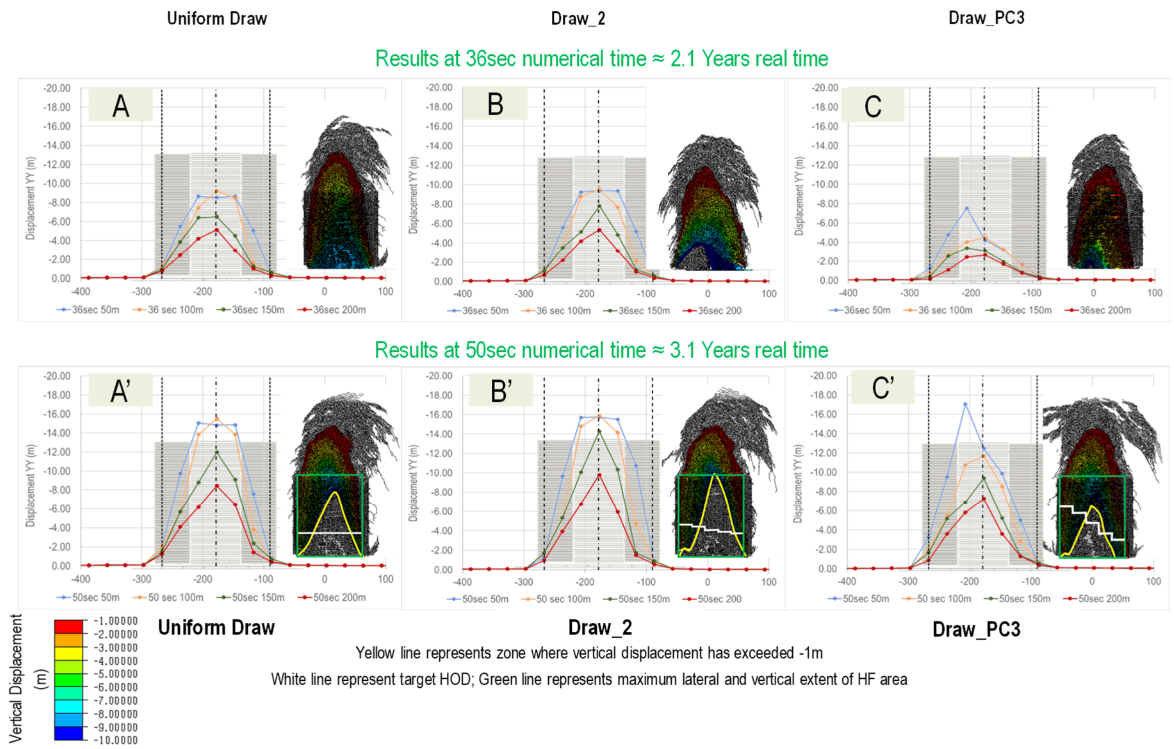

Figure 4 Vertical displacement plots for synthetic cave model (SCM) type H_L_H

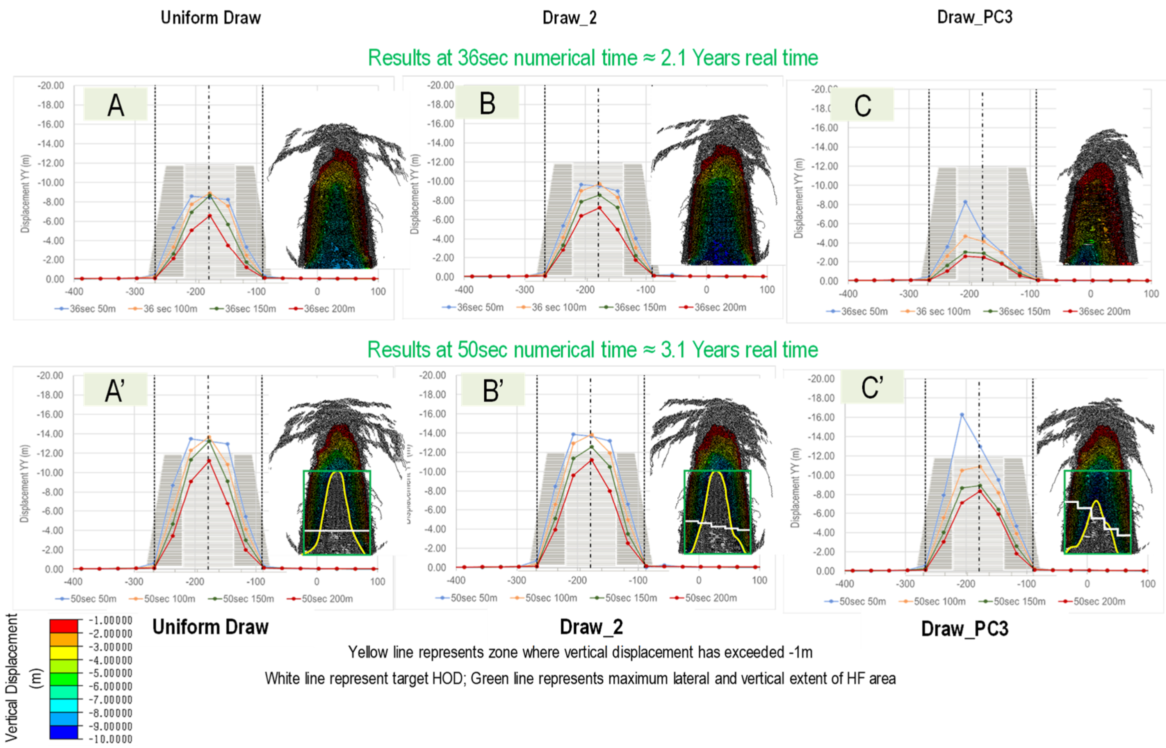

Figure 5 Vertical displacement plots for synthetic cave model (SCM) type HTP_L_HTP

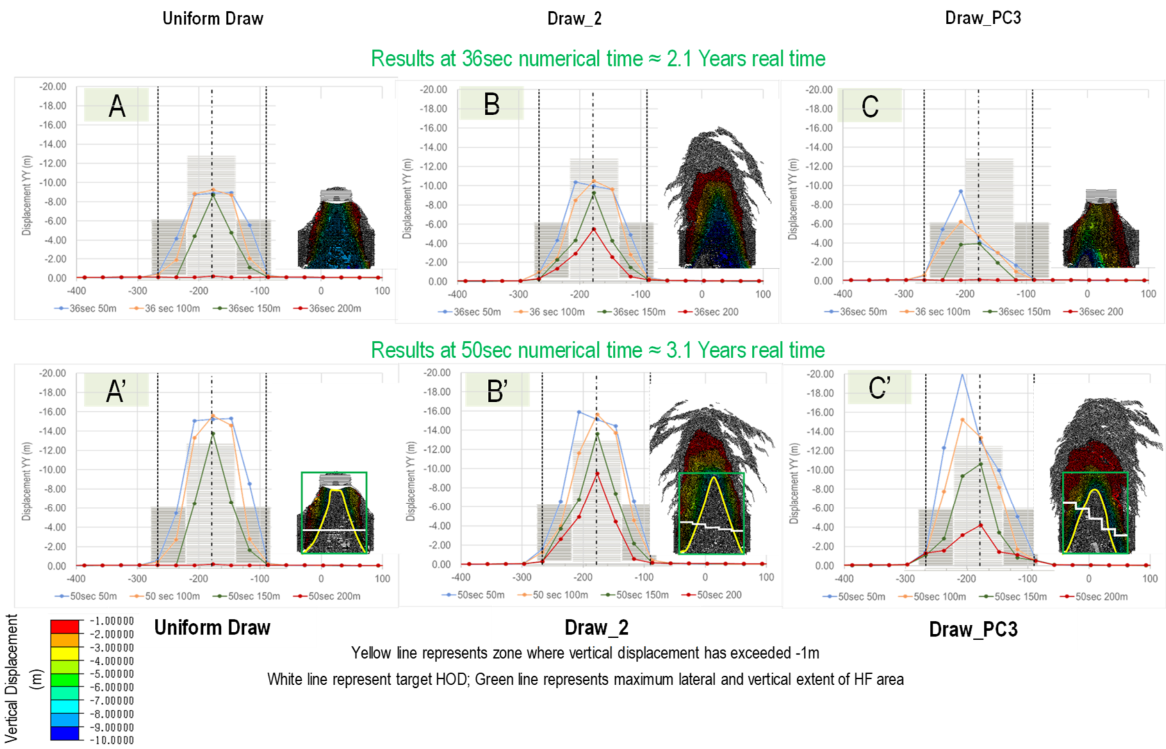

Figure 6 Vertical displacement plots for synthetic cave model (SCM) type H2_L_H2

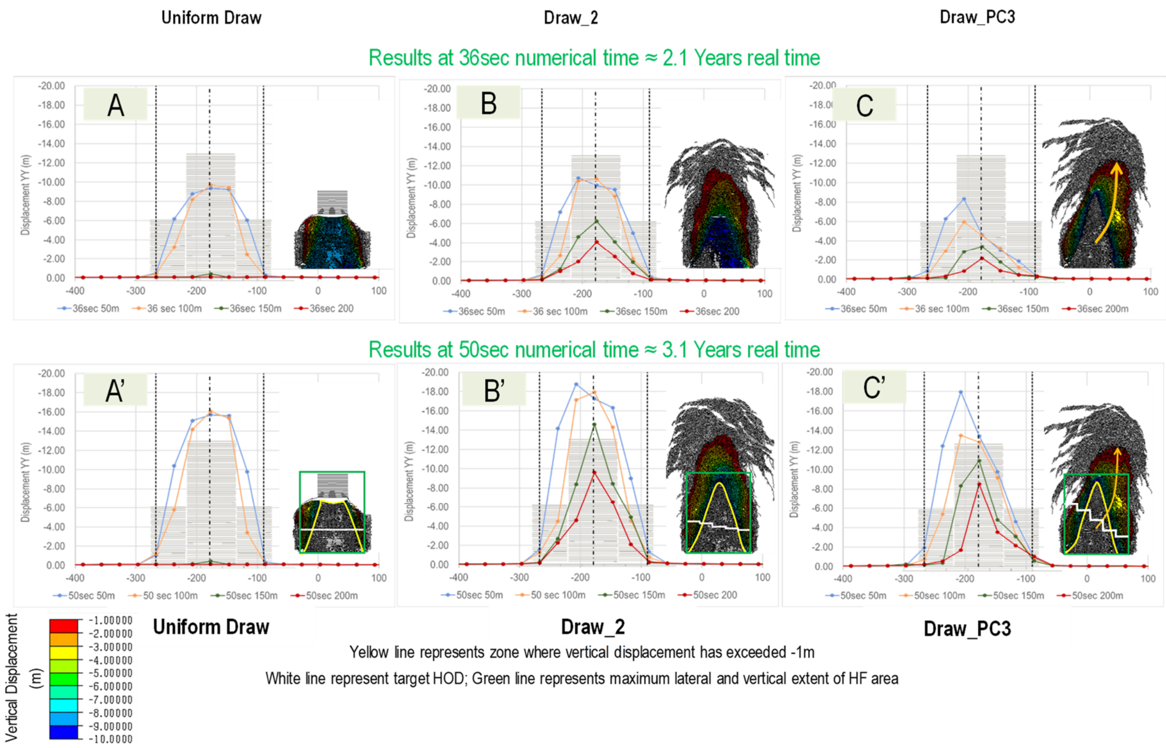

Figure 7 Vertical displacement plots for SCM type H2_L_H2 (top) and L2_L_L2 (bottom)

3.3 Analysis of caving rates

Caving rates for the 15 different models are estimated with respect to the value of preconditioning intensity, measured by the average areal fracture intensity (P_{21}), which is defined as the total trace length of the fractures per mapped area, for HF for each model. The P_{21} for each model is weighted to account for the different HF intensity along the flanks and core. Caving rates are calculated for each model using the following procedure: i) only history points within the undercut region are used to assess rates; ii) a history point is defined as being active once it meets the caving threshold (assumed as -1 m displacement); and iii) caving rate is the measured, using Equation 1, as the relative velocity required to have at predefined number of history points active on selected elevations.

$$Caving\ rate\ = \frac{[difference\ in\ height\ of\ monitoring\ points]}{[Time\ for\ a\ selected\ number\ of\ monitoring\ points\ to\ have\ caved]} \times [conversion\ to\ real\ time] \qquad (1)$$

In Equation 1, the selection of the number of history points is a critical parameter that affects the simulated caving rates. A high caving rate cannot be taken as an indicator of a well-developed cave if the caving rate is measured for a single point or a limited series of points above the undercut. Caving rates should be measured along regular intervals across the footprint in order to better characterise possible plug flow mechanics or asymmetrical cave development. The authors suggest using a minimum number of history points such that their distance is less than ¼ of the maximum width of the undercut area. This procedure provides a reasonable 'averaged' caving rate across the undercut. Accordingly, four monitoring points were used in the current models to calculate caving rates. The modelling results show that caving rates are controlled by a combination of preconditioning and draw strategies (Figure 8).

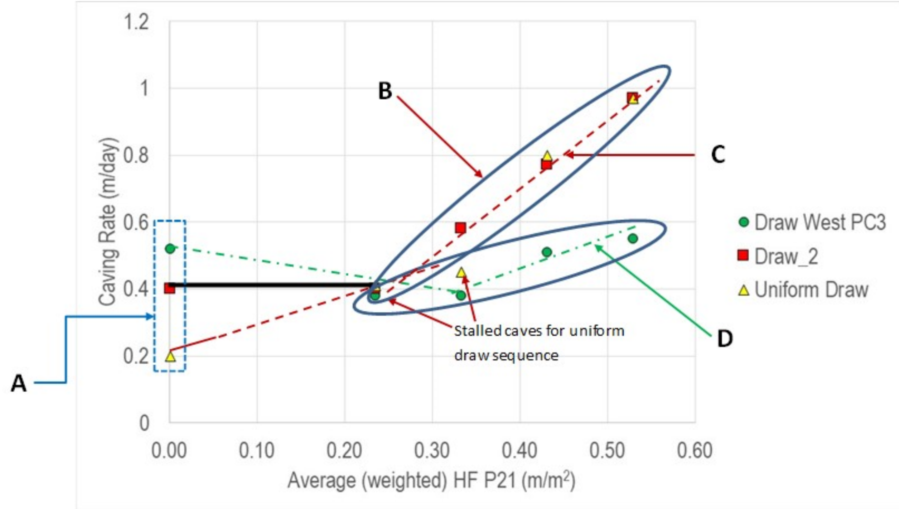

Figure 8 Relationship between caving rates and areal fracture intensity of the preconditioning fractures (HF P21). See text for explanation attached to labels A, B, C and D

The results suggest that adopting a non-uniform preconditioning strategy will not necessarily result in better caving rates compared to those estimated for naturally fractured rock masses (Label A, Figure 8). In addition, only when a draw sequence is adopted that reduces the risk for cave stall a relationship can be found between HF intensity and caving rates (Label B, Figure 8). A relatively high areal fracture intensity (P_{21}) is required for a uniform draw sequence to have a positive impact on caving rates (Label C, Figure 8). Furthermore, for highly asymmetrical draw sequences, the caving rate would not increase as expected even in the presence of a well-preconditioned zone (Label D, Figure 8).

4 Large-scale synthetic cave models

The cave models presented in Section 3 are robust in terms of run times due to their down-scaled dimensions of the built undercut and the extent of the preconditioning area. The shorter run times compared to those likely required for larger cave models with actual dimensions provides the opportunity to investigate several HF scenarios, draw sequences and consequently assist in narrowing down the selection of the optimised preconditioning and draw strategies to be implemented in larger mine scale models. In the Section the authors present the results of larger cave models, which simulate the design depth and dimensions of the proposed lift of an operating cave mine. The large-scale SCM simulate the design depth and dimensions of a planned undercut (1,410 m deep, 300 m long) in which the height of the preconditioning is 600 m. Geological faults are also included in the model. The large-scale SCM models adopts the same draw approach described in the previous section. The topography, lateral boundaries, and lateral constraints are the same as those used in the back-analysis of an undisclosed cave mine in Australia. Five models with different precondition fracture patterns were considered (Figure 9).

The results (Figure 10) indicates that in the absence of preconditioning, caving would be influenced by faulting, which would cause a relatively large portion of the rock mass along the eastern flank to undergo minor fragmentation with limited mobilisation. These observations become clear when comparing the results of the model without preconditioning and the models with either a slightly or aggressive draw strategies and the proposed PC2-3 HF design or alternative uniform HF strategies. As shown in Figure 10 ([2] and [3]), extending the HF pattern outside on each side of the undercut would be beneficial in mobilising the flanks when the slightly asymmetric draw is applied. However, applying a more aggressive asymmetric draw (see Figure 10, [3]) could potentially adversely influence cave mobilisation on the flanks with reduced cave growth. This result highlights the importance of looking at the combination of the HF patterns and applied draw strategy as a mechanistic system that controls the cave shape development. With respect to impacts of higher density of the HF (preconditioning spacing), it appears that within the same period (three years), a reduced cave advance is achieved in the simulations when a larger HF spacing is introduced in the models (see Figure 10, [4], and [6]). In terms of inhomogeneity in distribution of the HF, the modelling results presented in Figure 10, [5] indicates that the importance of introducing a uniform preconditioning pattern in order to avoid loss of recovery in the situation where the part of the rock mass above the undercut is not properly preconditioned due to both local conditions (e.g. fracture initiation in conductive shear and fault zones) and operational issues.

The calculated caving rates are shown in Figure 10. Comparison between the calculated caving rates indicates that limited difference in caving rates is measured when considering a large cave front (seven monitoring points); Differences only become apparent when considering a narrow cave front (four monitoring points). This behaviour may be explained by taking into consideration three important factors:

1. The larger size of the undercut and the lack of drawpoints pillars favours an overall plug flow, which is larger at centre of the drawzone. This somehow reduces the impact of HF intensity.
2. The assumed HF patterns are geometrically similar (except for [5] in Figure 10).
3. The comparison between models does not include the tonnes produced, rather it refers to the Target HOD imposed by the assumed draw sequence.

The results also show that for a narrow cave front (4 monitoring points), a reduction in preconditioning intensity corresponds to a reduced caving rate. With respect to the models with a slightly asymmetric draw sequence, the base case model with no preconditioning is the slowest in terms of cave growth rate (see the values of average caving rates in Figure 11). From a cave rate perspective, the uniform HF pattern appears more favourable than pattern with a tapered eastern flank (Tapered_HF). The presence of a zone (gap) of missing HF results in a caving rate reduction, which becomes larger as the cave front is reduced in proximity of the gap.

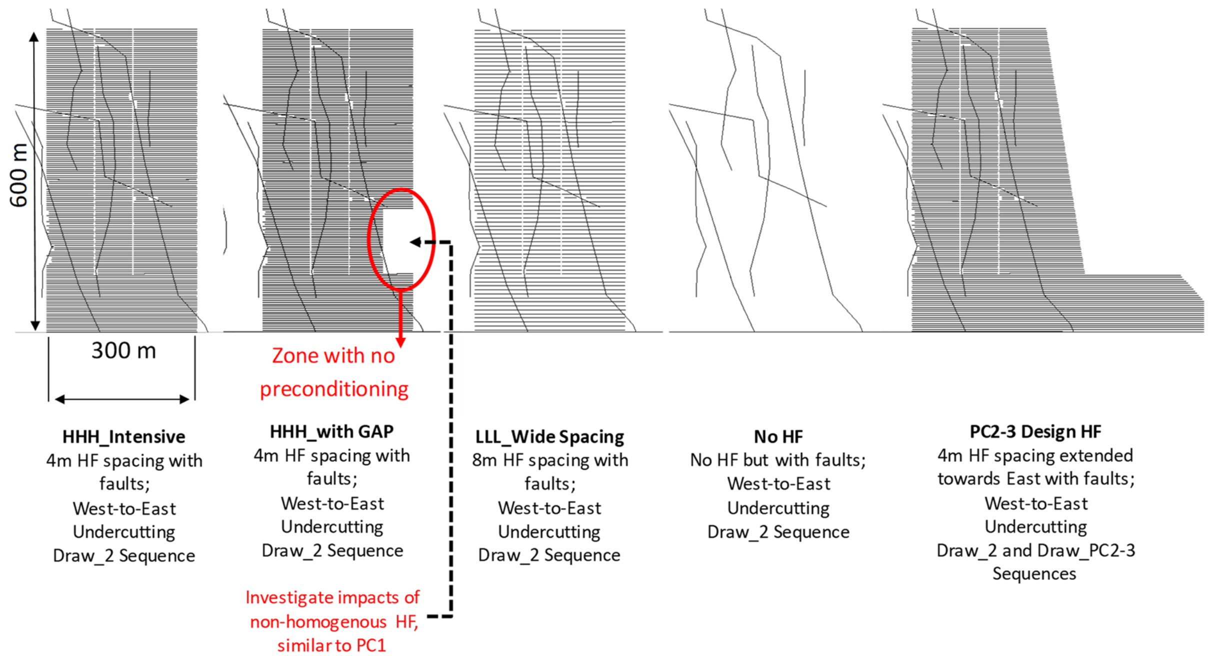

Figure 9 Geometry of preconditioning scenarios considered in the large-scale synthetic cave model, with specific reference to planned scenarios for an operating cave mine

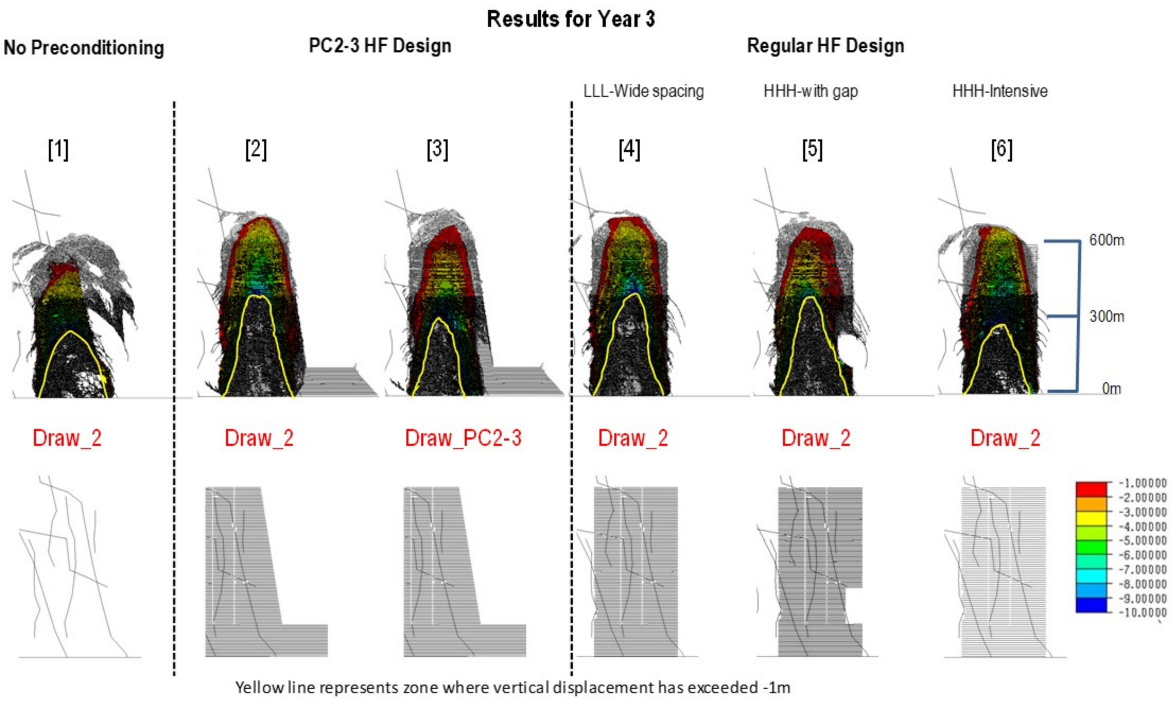

Figure 10 Cave development for different preconditioning scenarios

Models with 4 < Active History Points < 7

Height Above UCL (m)	No_HF	PC3_HF_Draw_2	PC3_HF_Draw_3	HHH	HHH_Gap	LLL
50	1.14	0.76	0.35	0.91	0.91	0.76
100	0.91	1.30	0.61	1.52	1.52	1.14
150	1.14	1.24	0.72	1.70	1.52	1.14
200	1.21	1.65	0.65	2.02	1.52	1.21
250	1.26	1.52	0.67	1.89	1.42	1.34
300	1.24	1.44	0.72	1.60	1.36	1.44
350	1.22	1.45	0.80	1.52	1.10	1.52
Average	1.16	1.34	0.64	1.59	1.33	1.22

Figure 11 Calculated caving rates for the large-scale synthetic cave model

5 Conclusion

This paper has presented the results of a modelling approach that can efficiently analyse cave initiation, cave propagation, effectiveness of preconditioning, draw sequence, and cave rates. An SCM approach is used to simulate stress-driven caving mechanisms. Testing a range of possible combination of HF configurations and draw strategy scenarios show that under specific circumstances preconditioning may have a detrimental impact on cave development. For example, a condition of cave stall could be generated for an otherwise caveable rock mass by preferentially channelling the cave through a high intensity preconditioning core. Tapered or uniform preconditioned flanks creates a strong boundary between preconditioned and in situ rock mass, which helps constraining the lateral extent of the cave shape (but preconditioning would need to marginally extend outside the undercut footprint).

Similarly, the results showed that applying a draw strategy that is aggressively pulling material in an asymmetric manner may cause a reduction in caving rates and generate asymmetrical cave development. This could have an impact in terms of dilution and ore recovery. Using a non-uniform draw strategy that gradually pulls material in an asymmetric manner could allow to circumvent potential cave stalling situations, and at the same time yield much higher rates of caving. This behaviour was further demonstrated in the large-scale SCM, in which a better cave development was achieved by drawing material preferentially on one of the cave flanks, thus creating a condition of asymmetric draw. The modelling results also indicate that preconditioning patterns need to be as uniform as possible (this is not practical nor realistic, it is more academic comment), with the consequence of less well preconditioning zones being clearly seen in reduced caving rates and reduced recovery. It is recognised that often HF development is challenging where conductive fault zones are encountered. As mentioned above, failure to provide a homogeneous fabric may result in an outcome like the PC1 inclined flank.

Despite their conceptual nature, the proposed modelling approach was capable to demonstrate the interdependence of preconditioning and the adopted draw sequence. This has clear implications for cave design as it further confirms the complexity of caving mechanics is such that treating parameters in isolation (preconditioning, sequence of undercutting and draw strategy) may lead to flawed conclusions with respect the impact of rock mass preconditioning. There is no doubt that 3D models are better than 2D at capturing stress evolution around a cave, but we should not forget the fact that numerical models for rock engineering application still rely on rather empirical and subjective methods to define rock mass properties (Elmo et al. 2022; Elmo & Stead 2021). According to those authors there is a cognitive resistance to accept that rock mass quality does not represent a measurement of well-defined physical rock mass properties and attempts to quantity it only provides an illusion of accuracy.

Acknowledgement

The authors acknowledge Newcrest Mining for their support, collaboration, and permission to publish this paper.

References

Beck, D & Pfitzner, M 2008, 'Interaction between deep block caves and existing, overlying caves or large open pits', *Proceedings of the 5th International Conference and Exhibition on Mass Mining (MassMin2008)*, Luleå University of Technology, Luleå, pp. 381–391.

Beck, DA & Putzar, G 2011, 'Coupled flow-deformation simulation for mine scale analysis of cave initiation and propagation' *Proceedings of the 12th ISRM Congress*, International Society for Rock Mechanics and Rock Engineering, Lisbon.

Bieniawski, Z 1989, *Engineering Rock Mass Classifications: A Complete Manual for Engineers and Geologists in Mining, Civil, and Petroleum Engineering*, John Wiley and Sons, Hoboken.

Borges, JL 1946, 'On Exactitude in Science', Los Anales de Buenos Aires, vol. 3.

Brzovic, A & Villaescusa, E 2007, 'Rock mass characterization and assessment of block-forming geological discontinuities during caving of primary copper ore at the El Teniente mine, Chile', *International Journal of Rock Mechanics and Mining Sciences*, vol. 44, no 4, pp. 565–583.

Deere, DU, Merritt, AH & Coon, RF 1969, E*ngineering classification of in-situ rock*, technical report AFWL-TR-67-144, Air Force Weapons Laboratory, Air Force Systems Command, Kirtland Air Force Base, New Mexico.

Elmo, D, Stead, D & Rogers, S 2008, 'Quantitative analysis of a fractured rock mass using a discrete fracture network approach: Characterisation of natural fragmentation and implications for current rock mass classification systems', *Proceedings of the 5th International Conference and Exhibition on Mass Mining (MassMin2008)*, Luleå University of Technology, Luleå, pp. 1023–1032.

Elmo, D, Rogers, S, Beddoes, R & Catalan, A 2010, 'An integrated finite/discrete element method – discrete fracture network synthetic rock mass approach for the modelling of surface subsidence associated with panel cave mining at the Cadia East underground project', in Y Potvin (ed.), *Caving 2010: Proceedings of the Second International Symposium on Block and Sublevel Caving*, Australian Centre for Geomechanics, Perth, pp. 167–179, https://www.doi.org/10.36487/ACG_rep/1002_9_Elmo

Elmo, D, Vyazmensky, A, Stead, D & Rogers, S 2012, 'Applications of a finite discrete element approach to model block cave mining', in L Ribeiro e Sousa, E Vargas, MM Fernandes & R Azevedo (eds), *Innovative Numerical Modelling in Geomechanics*, 1st edn, pp. 355–371.

Elmo, D, Rogers, S, Dorador, L & Eberhardt, E 2015, 'An FEM-DEM numerical approach to simulate secondary fragmentation', *Computer Methods and Recent Advances in Geomechanics: Proceedings of the 14th International Conference of International Association for Computer Methods and Recent Advances in Geomechanics*, Taylor & Francis Books Ltd, Milton Park, pp. 1623–1628

Elmo, D & Stead, D 2021, 'The role of behavioural factors and cognitive biases in rock engineering', *Rock Mechanics and Rock Engineering*, vol. 54, no. 1, pp. 1–20, https://www.doi.org/10.1007/s00603-021-02385-3

Elmo, D, Mitelman, A & Yang, B 2022, 'An examination of rock engineering knowledge through a philosophical lens', *Geosciences*, vol. 12, no. 174, https://www.doi.org/10.3390/geosciences12040174

Hoek, E 1999, 'Putting numbers to geology—an engineer's viewpoint', *Quarterly Journal of Engineering Geology and Hydrogeology*, vol. 32, no. 1, pp. 1–19.

Mitelman, A 2020, *Derivation of an Equivalent Boundary Method for Ground Interaction Problems*, PhD thesis (unpublished), The University of British Columbia, Vancouver.

Owen, DRJ, Feng, YT, de Souza Neto, EA, Cottrell, MG, Wang, F, Andrade Pires, FM & Yu, J 2004, 'The modelling of multi-fracturing solids and particulate media', *International Journal for Numerical Methods in Engineering*, vol. 60. pp. 317–339.

Pine, RJ, Owen, DRJ, Coggan, JS & Rance, JM 2007, 'A new discrete modelling approach for rock masses', *Geotechnique*, vol. 57, no. 9, pp 757–766.

Rogers, S, Elmo, D, Webb, G & Catalan, A 2014, 'Volumetric fracture intensity measurement for improved rock mass characterisation and fragmentation assessment in block caving operations', *Rock Mechanics and Rock Engineering*, vol. 48, no. 2, pp. 633–649.

Sainsbury, D, Sainsbury, B, Board, M & Loring, D 2011, 'Numerical back analysis of structurally controlled cave initiation at propagation at the Henderson Mine', in AT Innacchione, GS Esterhuizen & AN Tutuncu (eds), *Proceedings of the 45th US Rock Mechanics/Geomechanics Symposium*, American Rock Mechanics Association, Alexandria.

Sainsbury, B, Sainsbury, D & Carroll, D 2018, 'Back-analysis of PC1 cave propagation and subsidence behaviour at the Cadia East mine', in Y Potvin & J Jakubec (eds), *Caving 2018: Proceedings of the Fourth International Symposium on Block and Sublevel Caving*, Australian Centre for Geomechanics, Perth, pp. 167–178, https://www.doi.org/10.36487/ACG_rep/1815_10_Sainsbury

Shapka-Fels, T & Elmo, D 2022, 'Numerical modelling challenges in rock engineering with special consideration of open pit to underground mine interaction', *Geosciences*, vol. 12, no. 5, https://www.doi.org/10.3390/geosciences12050199

Vyazmensky, A 2008, *Numerical Modelling of Surface Subsidence Associated with Block Cave Mining Using a Finite Element/Discrete Element Approach*, PhD thesis, Simon Fraser University, Burnaby.

Vyazmensky, A, Elmo, D & Stead, D 2009a, 'Role of Rock mass fabric and faulting in the development of block caving induced subsidence', *Rock Mechanics and Rock Engineering*, vol. 43, https://www.doi.org/10.1007/s00603-009-0069-6

Vyazmensky, A, Stead, D, Elmo, D & Moss, A 2009b, 'Numerical analysis of block caving-induced instability in large open pit slopes: a finite element/discrete element approach', *Rock Mechanics and Rock Engineerin*g, vol. 43, no. 1, pp. 21–39. https://www.doi.org/10.1007/s00603-009-0035-3